NASA
Technical
Paper
2469
C.2
May 1985

Adding Computationally Efficient Realism to Monte Carlo Turbulence Simulation

C. Warren Campbell

NASA

NASA Technical Paper 2469

1985

Adding Computationally Efficient Realism to Monte Carlo Turbulence Simulation

C. Warren Campbell

George C. Marshall Space Flight Center
Marshall Space Flight Center, Alabama

NASA
National Aeronautics and Space Administration

Scientific and Technical Information Branch

TABLE OF CONTENTS

LIST OF ILLUSTRATIONS

NOMENCLATURE

c	a parameter with absolute value between 0 and 1
coh_{ij}	coherence between ith and jth signals $S_{ij}^2/S_{ii}S_{jj}$
f	spatial or time frequency (m^{-1} or sec^{-1})
H_i	transfer function of filter between x_i and y_i
H_{ij}	transfer function of filter between y_i and y_j
L	length scale of turbulence (m)
s	Laplace transform s
S_{ij}	cross spectra between ith and jth signals
u_*	friction velocity
u_i	ith turbulent velocity component
x	a parameter with absolute value between 0 and 1
x_i	ith Gaussian white noise source
X_i	Laplace transform of x_i
y	lateral separation distance (m)
y_i	ith simulated time series
Y_i	Laplace transform of y_i
z_i	height above surface for ith signal (m)
σ_i	standard deviation of y_i

TECHNICAL PAPER

ADDING COMPUTATIONALLY EFFICIENT REALISM TO MONTE CARLO TURBULENCE SIMULATION

INTRODUCTION

The goal of Monte Carlo turbulence simulation is to provide turbulence for flight simulation. The presence of turbulence in pilot-in-the-loop simulations increases the pilot's workload as well as his sense of the realism of the simulation. A common complaint of pilots is that the turbulence provided is not realistic. The complaint is usually justified but not for the reason that the pilot believes. A real plane responds to turbulence in several ways. First, the random forces of lift and drag cause the center of gravity of the aircraft to translate in the three coordinate directions. Secondly, moments cause the craft to rotate about the roll, pitch, and yaw axes. Finally, the aircraft is an elastic body and the presence of aerodynamic forces and moments create a vibrational response in the airframe. The airframe "ringing" in many cases is a significant factor in creating the pilot perception of correct "feel." The incorrect "feel" is unlikely to arise from inaccuracies in the stochastic properties of the turbulence which are provided but, rather from aspects of aircraft response which are not modeled.

Of the three responses of the aircraft to turbulence mentioned above, only translation of the vehicle center of gravity is accounted for in common simulation practice. In some cases, only the vertical velocity component is simulated along the aircraft flight path. This turbulence component is typically simulated using explicit difference equations based on the Dryden spectral model, which is rational. Simulations comparing aircraft response to von Karman and Dryden turbulence were performed by Frost, et al. [1] and measurable differences were observed. These differences result from using less accurate rational models in generating one-dimensional turbulence. Roll and yaw moments cannot be realistically simulated unless variation of turbulent gusts across the body of the vehicle are simulated. Elastic airframe response cannot be simulated unless gust variation inputs are included.

Several investigators have attempted to add three-dimensionality to turbulence simulation. Tatom, et al. [2] simulated turbulent gusts and gust gradients. This approach assumes that at any instant, turbulent velocities vary linearly in any direction across the body of the aircraft. The turbulence was generated using a non-dimensional von Karman model approach and simulation by this model involves manipulation of a sizable data base. The assumption of linear velocity variation is not realistic, even for an aircraft of moderate size, as was shown in the NASA Gust Gradient Program [3]. Even so, in the opinion of the author, this approach is much better than simple one-dimensional models.

A highly accurate turbulence model which overcomes many conceptual difficulties was suggested by Campbell and Sandborn [4]. This technique combines remotely sensed atmospheric wind shear data with Monte Carlo generated three-dimensional turbulence. The problem with the model is that it requires the storage of a two-megabyte data base. Additionally, three-dimensional velocity cross correlations $[R_{uv}(x,y,z)]$ are not accounted for. At the present time, the technique would be useful only for large research simulators, but in the future as the cost of computer storage goes down, this or a derivative technique may be the method of choice. In any event, a long time will pass before any of the large air carriers will be willing to buy simulators with this kind of capability.

The facts concerning turbulence simulation are that simulator manufacturers are willing to add any capability to their simulators that simulator users are willing to buy. The users cannot afford to purchase high fidelity turbulence simulation capability unless high computational efficiency and low storage requirements come with it. Even as computers become faster, cheaper, and more capable the situation will not change as fast as the computers. The reason is that flight simulation model software increases in size as better computers become available, and the requirement for more realistic turbulence must compete with other requirements.

The purpose of this report is to document a concept which is an attempt to provide simulator users with three-dimensional turbulence simulation capability with a minimum increase in simulator computer demand. The concept is based on an earlier paper by Campbell [5], in which irrational von Karman spectra are approximated with rational functions. This approach is reviewed briefly in a later section, and its accuracy and computational advantages explained. The computational advantages of rational spectral models cannot be underestimated, and these will be explained in the next section.

MONTE CARLO TURBULENCE SIMULATION

The commonly applied engineering approach to Monte Carlo turbulence simulation is illustrated conceptually in Figure 1. Gaussian white noise is filtered by a linear filter whose filter function is chosen so that the spectrum of the output signal is the desired spectrum of turbulence. Because the filter is linear, the output signal is Gaussianly distributed. Some investigators use nonlinear filters (Reeves, et al. [6]) to better account for turbulent patchiness or other effects, but these techniques will not be considered here.

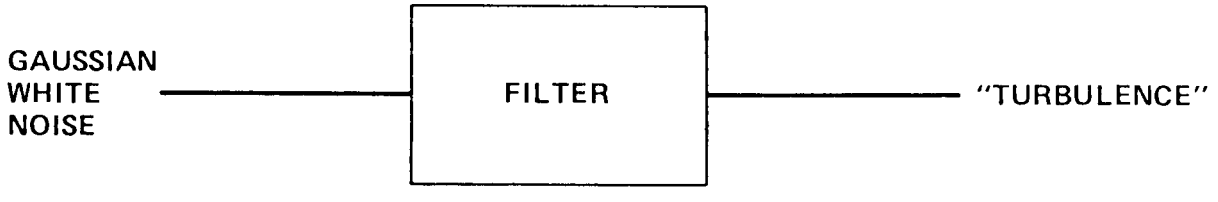

Figure 1. Monte Carlo turbulence simulation.

Figure 1 is a conceptual diagram and many different approaches may be used to achieve the simulated turbulence. The filter function may take the form of von Karman, Kaimal, Dryden, or other spectra. The Kaimal and von Karman spectra are irrational having a $f^{-5/3}$ falloff rate. The Dryden spectra fall off as f^{-2}. If irrational spectra are used, a block of noise must be generated, transformed to the frequency domain, multiplied point by point by the irrational filter function, and then inverse transformed back to the time domain. Spectral models based on rational functions can be used to generate explicit finite difference equations, i.e. reccursion relationships. The latter approach is computationally much more efficient than the use of FFT's for turbulence generation. For real time simulations where large blocks of mass storage are not available, the explicit difference equation approach is used almost exclusively. An understanding of the advantages of the rational versus the irrational approach is necessary to appreciate the technique proposed here, and the necessary explanations are given below.

The equations governing incompressible flow are the Navier-Stokes equations and the equation of continuity.

$$\partial u_i/\partial t + u_j \, \partial u_i/\partial x_j = -\frac{1}{\rho} \partial p/\partial x_i + \nu \, \partial^2 u_i/\partial x_j \partial x_j \tag{1}$$

$$\partial u_i/\partial x_i = 0 \tag{2}$$

The Navier-Stokes equations are nonlinear partial differential equations for which very few analytical solutions are known. They can be solved numerically, but direct turbulent simulation of flows with the high Reynolds numbers of the atmosphere is not now feasible, nor will it be in the forseeable future. Given these facts, how can a realistic atmospheric simuland be created? The answer is to use one-dimensional measurements of turbulent spectra to generate differential systems which when random noise is input, not so random noise with the required spectra are output. Consider for a moment, the Dryden spectrum for the longitudinal velocity component (Table 1). The s-domain filter function corresponding to this spectrum is given by

$$H_L(s) = a_1/(s + b_1) \tag{3}$$

$H_L(s) = Y(s)/X(s)$, where $X(s)$ is the transform of the input white noise, and $Y(s)$ is the transform of the filter output. Equation (3) can be rearranged as follows.

$$(s + b_1)\, Y(s) = a_1 X(s) \tag{4}$$

If the inverse Laplace transform is performed on equation (4), the result is an ordinary, first-order differential equation with constant coefficients.

$$dy/dt + b_1 y = a_1 x \quad . \tag{5}$$

Since b_1 is positive, this differential equation is stable since the filter function has only the one pole at $-b_1$ in the left half plane. Equation (5) can be discretized in many different ways, e.g. Runge-Kutta or predictor-corrector, but care must be taken that the resulting finite difference equations are also stable. Some commonly used discretizations do not satisfy this requirement, but Neuman and Foster [7] describe a scheme which guarantees that if the differential equation is stable the corresponding difference equation is stable.

The longitudinal filter function for the von Karman spectra is given in Table 1 and if manipulated as above the result is

$$(d_1 + s)^{5/6}\, Y(s) = c_1\, X(s) \tag{6}$$

TABLE 1. SPECTRA, TRANSFER FUNCTIONS, AND DIFFERENTIAL EQUATIONS CORRESPONDING TO THE DRYDEN AND VON KARMAN MODELS

DRYDEN

	LONGITUDINAL	LATERAL	VERTICAL
SPECTRA	$\phi_1 = \frac{\sigma_1^2 2L_1}{\pi} \frac{1}{1 + (2\pi L_1 f/V)^2}$	$\phi_2 = \frac{\sigma_2 L_2^2}{\pi} \frac{1 + 3(2\pi L_2 f/V)^2}{(1 + (2\pi L_2 f/V)^2}$	$\phi_3 = \frac{\sigma_3^2 L_3}{\pi} \frac{1 + 3(2\pi L_3 f/V)^2}{(1 + (2\pi L_3 f/V)^2}$
TRANSFER FUNCTIONS	$H_1(S) = \frac{C_1}{a_1 + S}$	$H_2(S) = \frac{C_2 (b_2 + S)}{(a_2 + S)^2}$	$H_3(S) = \frac{C_3 (b_3 + S)}{(a_3 + S)^2}$
ODE	$\frac{dy}{dt} + a_1 y = C_1 X$	$\frac{d^2y}{dt^2} + 2a_2 \frac{dy}{dt} + a_2^2 y = C_2 (\frac{dx}{dt} + b_2 x)$	$\frac{d^2y}{dt^2} + 2a_3 \frac{dy}{dt} + a_3^2 y = C_3 (\frac{dx}{dt} + b_3 x)$

VON KARMAN

	LONGITUDINAL	LATERAL	VERTICAL
SPECTRA	$\phi_1 = \frac{\sigma_1^2 2L_1}{\pi} \frac{1}{[1 + (2\pi a L_1 f/V)^2]^{5/6}}$	$\phi_2 = \frac{\sigma_2^2 L_2}{\pi} \frac{1 + 8/3 (2\pi a L_2 f/V)^2}{[1 + (2\pi a L_2 f/V)^2]^{11/6}}$	$\phi_3 = \frac{\sigma_3^2 L_3}{\pi} \frac{1 + 8/3 (2\pi a L_3 f/V)^2}{[1 + (2\pi a L_3 f/V)^2]^{11/6}}$
TRANSFER FUNCTIONS	$H_1(S) = \frac{C_1}{(a_1 + S)^{5/6}}$	$H_2(S) \frac{b_2 (S + C_2)}{(S + a_2)^{11/16}}$	$H_3(S) = \frac{b_3 (S + C_3)}{(S + a_3)^{11/16}}$
ODE	LINEAR, INFINITE ORDER ODE	LINEAR, INFINITE ORDER ODE	LINEAR, INFINITE ORDER ODE

Before, Y was multiplied by s whereas in the above equation, it is multiplied by an irrational factor. Multiplying by s is equivalent to taking the derivative in the time domain. For the case of an irrational factor, calculation of derivatives of fractional order must be determined which is a cumbersome process [8]. If derivatives of integer order are required, heuristically the irrational factor of Y(s) in equation (6) can be expanded in an infinite series. When transformed to the time domain, the result is a linear, ordinary differential equation of infinite order. Differential equations of infinite order cannot be discretized.

The spectra, transfer functions, and differential equations (where possible) for the Dryden and von Karman spectra are tabulated in Table 1. For the rational Dryden spectra, first or second order, linear, nonhomogeneous differential equations with random input can be derived. The corresponding difference equations are of the following form [9].

$$y_{n+1} = c_1 y_n + c_2 y_{n-1} + d_1 x_n + d_2 x_{n-1} \quad . \tag{7}$$

The calculation of an FFT requires a number of operations proportional to N $\log_2$N, where N is the number of points to be calculated. To generate N points of turbulence with an irrational spectrum requires the calculation of two FFT's and a point-by-point multiplication by the filter function. The total number of operations is then proportional to 2N $\log_2$N + 4N multiplications. For the above difference equation, the corresponding number of operations is 4N. If N = 1024, the number of multiplications is six times greater for the FFT approach. For larger values of N, the computational advantage becomes correspondingly greater. The computational advantage is actually greater than this because for the above difference equation, only four coefficients must be calculated while considerably more sines and cosines must be calculated in the FFT evaluations. The disadvantage of the Dryden model is its inaccuracy. In fact, the Dryden model can be considered a crude approximation to the more accurate Von Karman model. Campbell [5] has developed a new method which applies accurate, rational approximations to the von Karman spectra, and the result is simulated turbulence with rational spectra closely approximating the von Karman spectra. For the more complex transverse velocity component, 9N real multiplications are required to generate N points of turbulence. The computational efficiency is only 9/4 as large as for the Dryden model, and still holds a strong advantage over the FFT approach.

To this point, the only methods discussed that incorporate anything better than one-dimensional turbulence simulation were the studies by Tatom, et al. [2] and by Campbell and Sandborn [4]. The weaknesses of these two techniques were discussed. Other efforts which developed models for simulating multiple time series should be mentioned. To match coherence, Fichtl, et al. [10] summed and phase shifted a series of random noise inputs. The coherence matching only becomes exact in the limit as the number of random inputs approach infinity. Hoshiya and Tieleman [11] developed a method for two time series. This method requires summations of large numbers of sine and cosine terms. Neither of the two models are as computationally efficient as desired. In the following section, a method is proposed which uses rational approximations, and multipoint turbulence simulation with cross correlation to achieve three-dimensionality.

MULTI-POINT TURBULENCE SIMULATION

The problem addressed in this section is the generation of a number of time series with known spectra and cross spectra. Filter function forms will be developed for two series and for three series.

Generalizations to n dimensions will be apparent. The block diagrams will be developed in such a way that the form of the spectra and cross spectra of signals 1 and 2 will be the same whether only two signals or a hundred are being generated. Solution for the various filter functions in terms of the known spectra and cross spectra is thus simplified. Realizability of the required filter functions is another matter which cannot be presumed. For example, the product of a filter function and its complex conjugate must always be nonnegative. For some simulation situations negative values may be required to satisfy relationships between transfer functions and signal spectra and cross spectra. The question of realizability will be addressed briefly in this section.

A block diagram which permits the generation of two time series with given spectra and cross spectrum is depicted in Figure 2. The indicated filter functions are unknown, i.e. H_1, H_{12}, and H_2. These are to be found in terms of S_{11}, S_{12}, and S_{22}, which are known quantities. Assuming that the Gaussian white noise inputs, x_1 and x_2, are independent and have unit variance, the three spectra are given by the following equations.

$$S_{11} = |H_1|^2 \tag{8}$$

$$S_{12} = H_{12}\, S_{11} \tag{9}$$

$$S_{22} = |S_{12}|^2/S_{11} + |H_2|^2 \tag{10}$$

Equations (8), (9), and (10) when solved yield the required values for $|H_1|^2$, H_{12}, and $|H_2|^2$. Solutions for H_1 and H_{12} are obvious. The solution for $|H_2|^2$ is more interesting.

$$|H_2|^2 = S_{22} - |S_{12}|^2/S_{11} = S_{22}\,(1 - \mathrm{coh}_{12}(f)) \quad . \tag{11}$$

The question of realizability arises here in connection with $|H_2|^2$. Equation (11) reveals that a negative value of $|H_2|^2$ is not possible since S_{22} is positive and the coherence varies between 0 and 1.

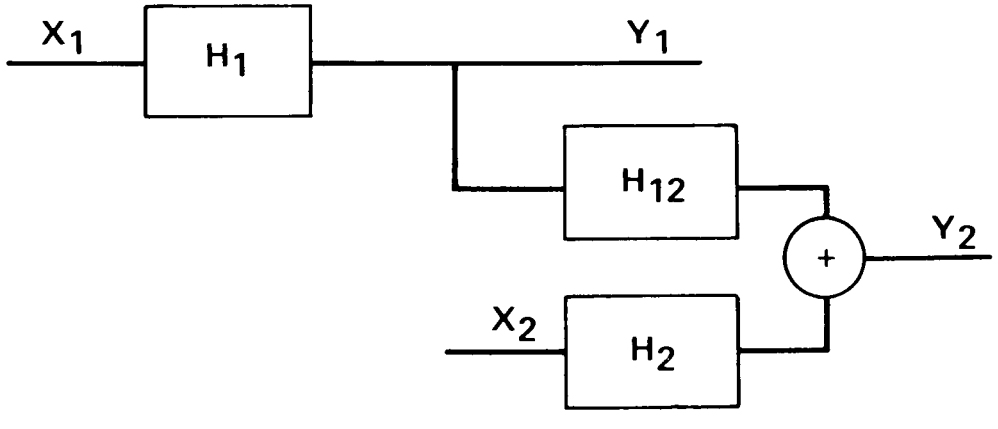

Figure 2. Block diagram for generating two correlated time series.

Figure 3 depicts the block diagram for the three time series case. In the figure all information flows from top to bottom, i.e., y_1 influences y_2 and y_3, and y_2 influences y_3, but y_1 is not affected by y_3 or y_2 and so on. The one way flow of information means that values of H_1, H_{12}, and H_2 keep the same form that they had in the two signal case and as was given in equations (8) to (11). For the three signal case, only solutions of H_{13}, H_{23}, and H_3 must be obtained. The results of the solutions are given below.

$$H_{13} = (S_{13}S_{22} - S_{12}S_{23})/DEL \tag{12}$$

$$H_{23} = (S_{11}S_{23} - S_{21}S_{13})/DEL \tag{13}$$

$$|H_3|^2 = (S_{11}S_{22}S_{33} + S_{12}S_{23}S_{13} + S_{13}S_{21}S_{32} - S_{11}|S_{23}|^2 - S_{33}|S_{12}|^2 - S_{22}|S_{13}|^2)/DEL \tag{14}$$

where $DEL = S_{11}S_{22} - |S_{12}|^2$. DEL is always nonnegative.

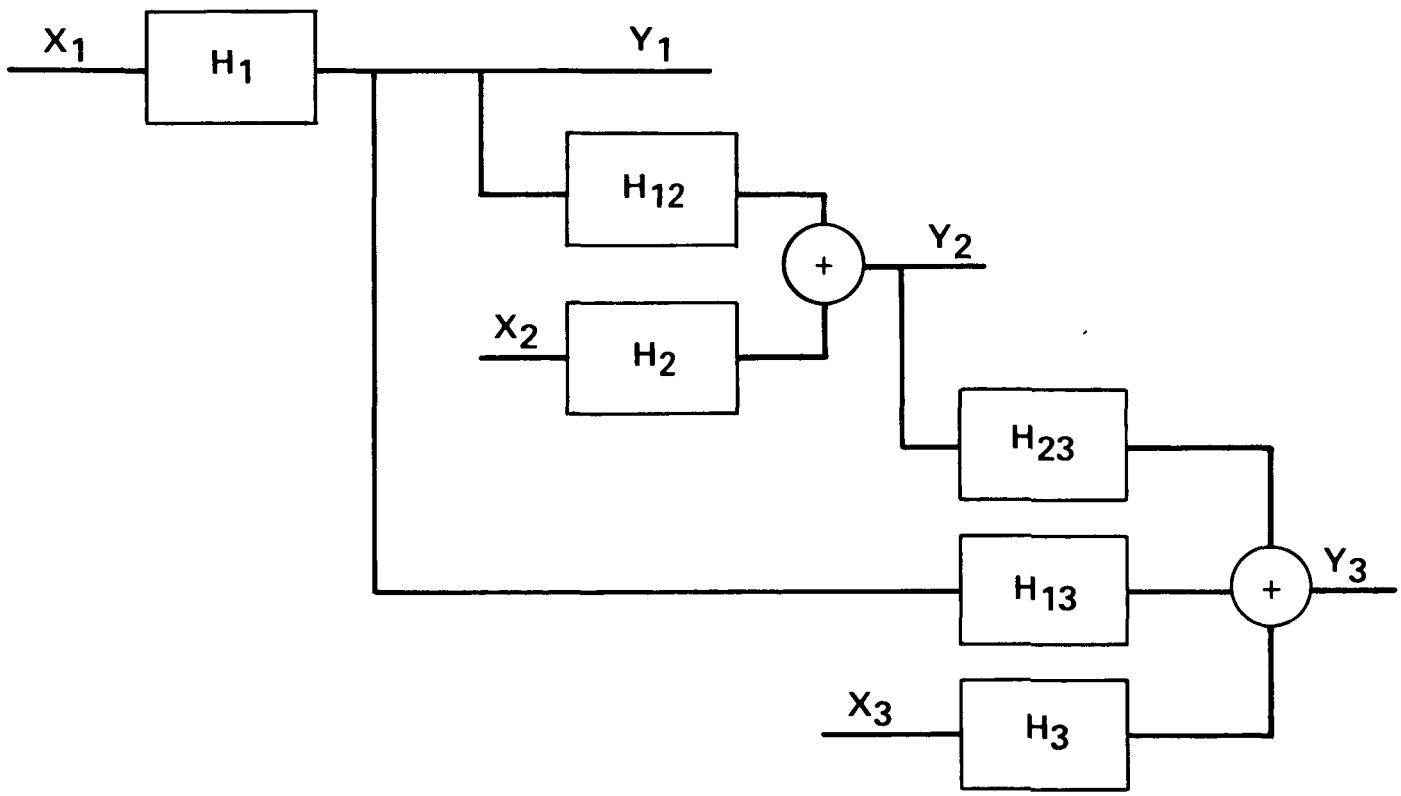

Figure 3. Block diagram for simulating three correlated time series.

Realizability questions arise with regard to $|H_3|^2$. The value of this quantity could conceivably become negative. The numerator of equation (14) is the determinant $[S_{ij}]$. Since equations (8) to (11) indicate that all the principle minors of rank one and two are nonnegative, a nonnegative value of the

determinant S_{ij} means that the matrix would be positive definite. The matrix S_{ij} is Hermitian, i.e., $S_{ij} = S_{ji}^*$. A nonrealizable example can be generated.

$$|H_3|^2 = \begin{vmatrix} 1 & x & cx \\ x & 1 & x \\ cx & x & 1 \end{vmatrix} / \text{DEL} \quad . \tag{14}$$

The parameters, c and x have values between -1 and 1. For a positive value of $|H_3|^2$, the above determinant must be positive. The parameters are functions of frequency, but we are searching for negative values of the right side of equation (14) at only one frequency. The physical picture relating to equation (14) is that of three time histories recorded from an aircraft flying through isotropic turbulence (Fig. 4). The points are equally spaced so that $S_{12} = S_{23} = x$. The cross spectra between the nonadjacent points, $S_{13} = cx$. If the determinant in the above equation is evaluated, the result is given as follows.

$$\text{Det}(S_{ij}) = 1 + 2x^3c - 2x^2 - c^2x^2 \quad . \tag{15}$$

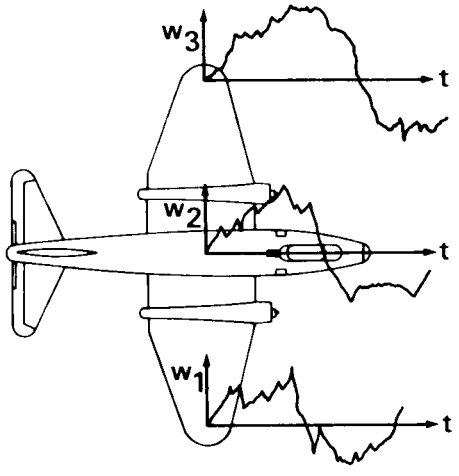

Figure 4. Physical example of simulation of three series at uniformly spaced points.

For realizability, the determinant must be nonnegative. Regions of x-c space where the determinant is positive or negative may be specified by finding the curve where the determinant is zero. The above expression is quadratic in c and curves of zero value of the determinant are given by $c = 1/x$ and $c = (2x^2 - 1)/x$. Regions of negative value for equation (15) are indicated in Figure 5. Although the c-x plane is shown for large positive and negative values of x and c, in reality x and c only vary in absolute value between zero and one. The nonrealizable values in the c-x plane occur for x large, or for small separations of the three points of Figure 4 relative to the length scale of turbulence. Values of H_3 were calculated for these small separations, and indeed computer errors related to negative square roots were encountered. Realizable transfer functions for larger separations are shown for different separations in the next section.

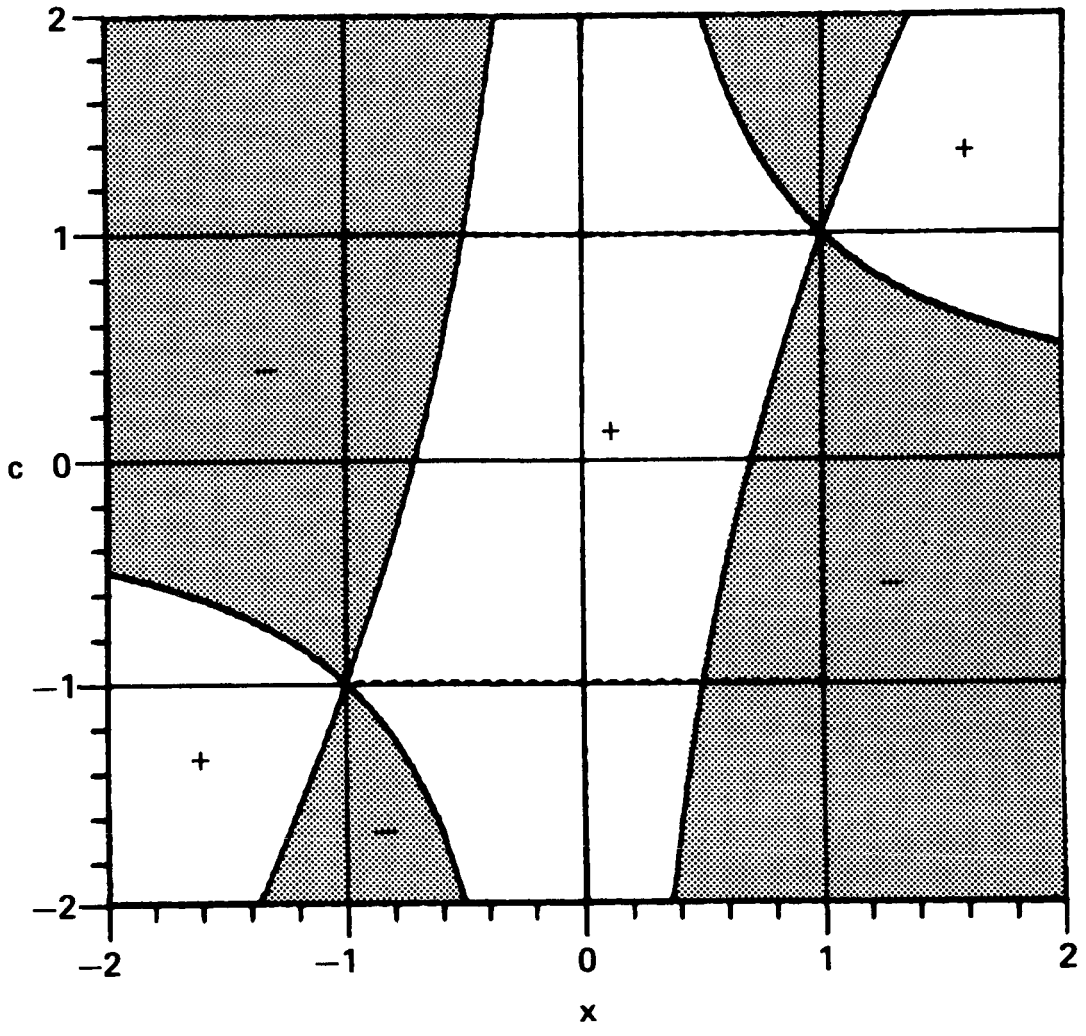

Figure 5. Three time series realizability in c-x space.

The block diagrams shown in Figures 2 and 3 indicated a method of generating two and three time series with desired spectra and cross spectra. The extension to any number of series is straight forward and will not be presented here. Future research along these lines should be directed toward gaining an understanding of restrictions under which realizability is satisfied. Systems other than the ones presented here for generating correlated random signals might be discovered which assure realizability.

In the preceding section, the Von Karman approximant (VKA) method [5] for approximating irrational spectra was described. In this section, forms of transfer functions suitable for generating correlated signals was described. The VKA method in combination with the transfer function forms presented here can provide a computationally efficient means for inserting three-dimensionality into Monte Carlo turbulence simulation. In the next section, example transfer functions for realistic situations will be shown.

EXAMPLE TRANSFER FUNCTIONS

Turbulence encountered by an aircraft at altitude can be modeled as isotropic. Assuming the validity of Taylor's frozen turbulence hypothesis and Von Karman turbulence, the cross spectra of the vertical velocity component was calculated by Houbolt and Sen [12]. Their expression for the cross spectrum is given in the following equation.

(16)

In the above expression, K_a is the modified Bessel function of the second kind. Values of this function for a = 5/6 and 11/6 were obtained using a subroutine, BESSKA available from the National Center for Atmospheric Research (NCAR). Values for the transfer functions H_1, H_{12}, H_2, H_{13}, H_{23}, and H_3 are plotted in Figures 6 and 7. Figure 6 corresponds to a point spacing of y/L = 0.2, and 0.4. Figure 7 is a corresponding plot for y/L = 0.05, and 0.1. For each of these separations H_3 is realizable, but for some smaller separations, it is not. These transfer functions are suitable for flight simulations at altitude where turbulence is more nearly isotropic.

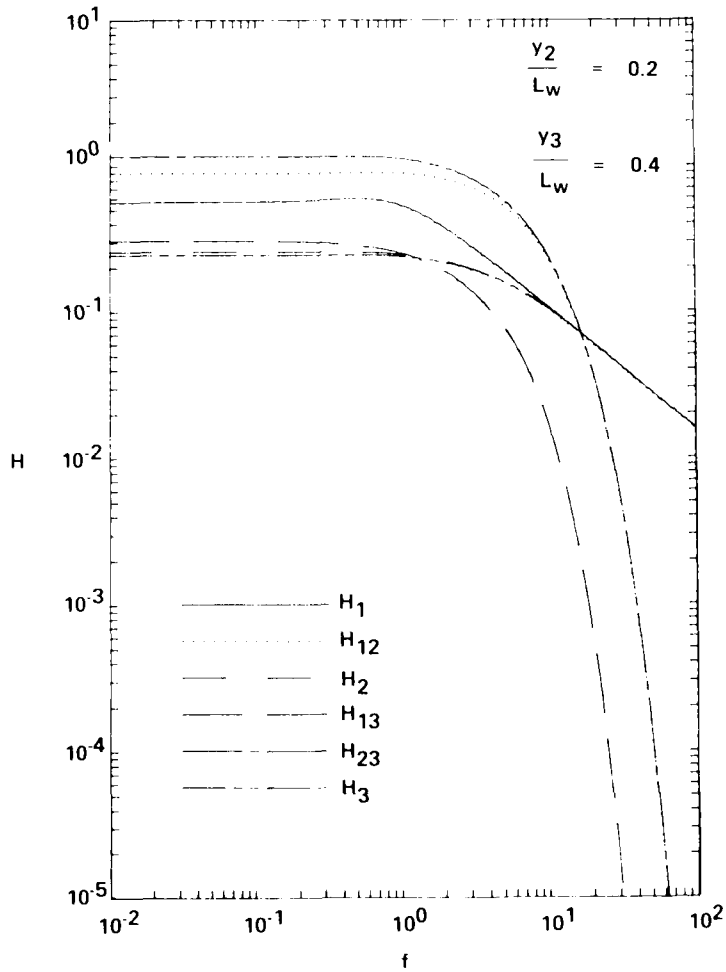

Figure 6. Three series transfer functions for vertical velocities with spacing y/L = 0.2 and 0.4.

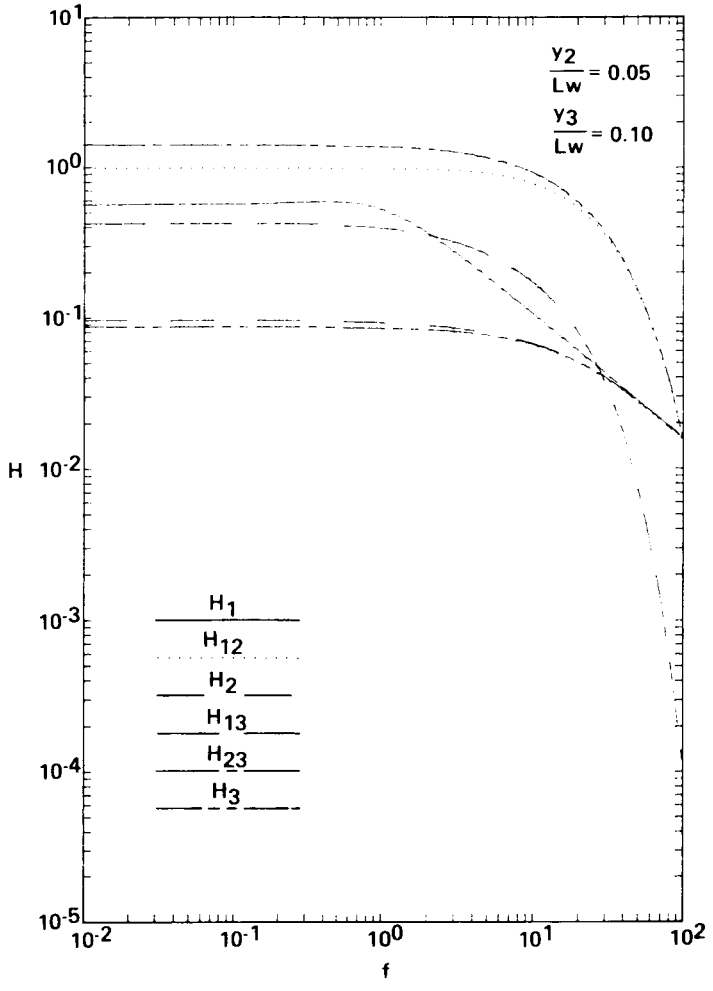

Figure 7. Three series transfer functions for vertical velocities with y/L = 0.05 and 0.1.

For flight at low altitude, an exponential form of the cross spectra is generally used. A nice summary of coherence functions in the lower atmosphere is given by Panofsky and Dutton [13]. The cross spectra used for demonstration purposes here is valid for the Cape Canaveral, Florida area. The form is taken from Fichtl, et al. [14].

$$S_{im} = \sqrt{S_{ii}S_{mm}}\ \exp\left(-0.3465\ \Delta f/\Delta f_{0.5} + j2\pi g\Delta f\right) \tag{17}$$

where $\Delta f = 2\pi f(z_m/u_m - z_i/u_i)$.

$f_{0.5} = 0.00573$ for the longitudinal component in strong winds.

$g = 0.7$ for longitudinal component and the average of z_i and z_m are less than 100 m.

z_i = height above the ground.

For the purpose of demonstration, z_1 = 10 m, z_2 = 20 m, and z_3 = 30 m were selected. Using the logarithmic velocity profile and an assumed value of the friction velocity u_* = 0.59, u_1 = 9.17 m/s, u_2 = 10.18 m/s, and u_3 = 10.79 m/s were calculated based on a typical roughness length of 0.02 m. S_{ii} was assumed to be in the form of the Von Karman spectrum for longitudinal velocity. Typical values of L_1 = 21.4 m, L_2 = 33.3 m, and L_3 = 42.9 m were used. Gust standard deviations, σ_1 = 1.185 m/s, σ_2 = 1.517 m/s, and σ_3 = 1.75 m/s were calculated from information given by Tatom, et al. [2]. The corresponding, realizable transfer functions are plotted in Figure 8. Interestingly, because of the large separations, and the fact that turbulent length scales increase as a fraction of height in lower planetary boundary layer (PBL), the transfer functions H_{ij} are very much smaller than the H_i. That being the case, for unrealizable solutions, the separations must be very small indeed to run into nonrealizability problems.

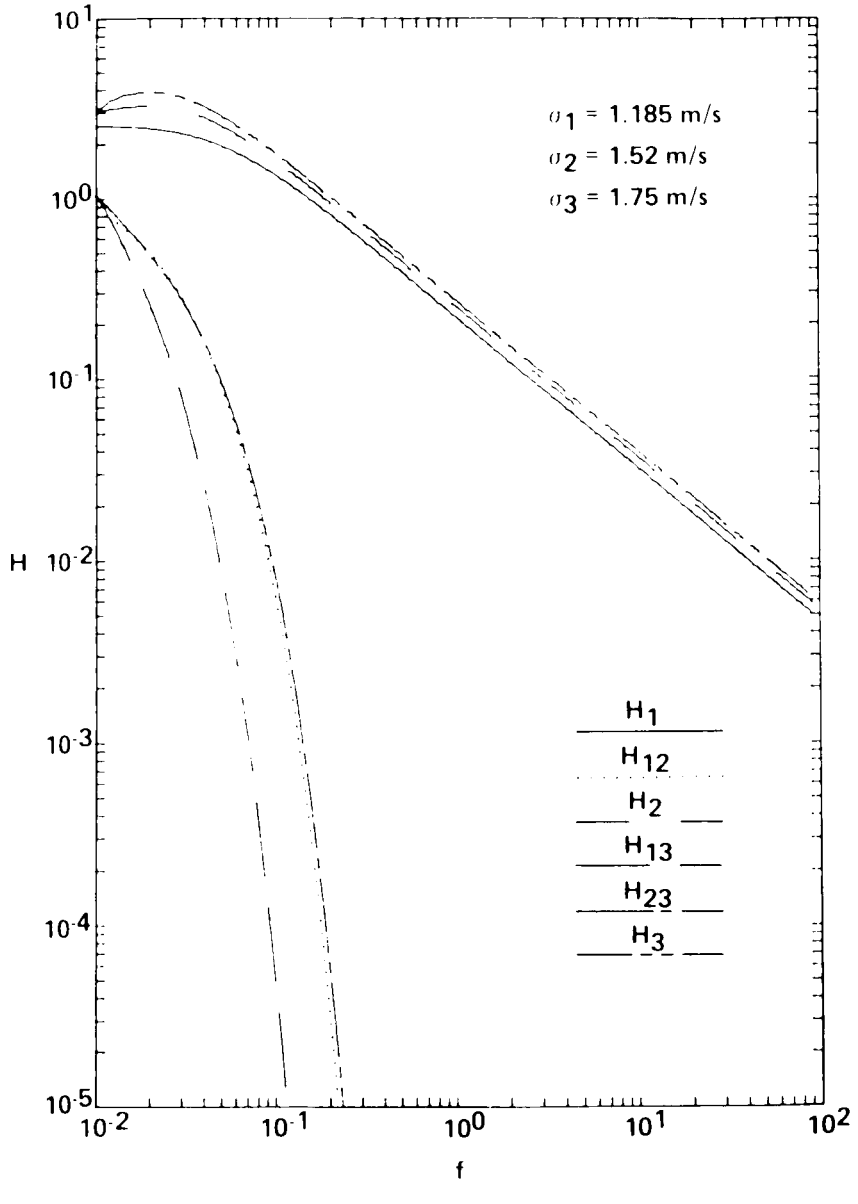

Figure 8. Three series transfer functions for longitudinal velocities and vertical separations (z_1 = 10 m, z_2 = 20 m, z_3 = 30 m).

Another example which is interesting to consider is that of three dimensional, isotropic turbulence. The idea here is to generate three three-dimensional signals with given spectra and cross spectra. This is the most general simulation possible and would contain all one-dimensional cross spectra. The spectra in general must be in the following form.

$$S_{ij} = E(f)\ (f^2\ \delta_{ij} - f_i f_j)/4\pi f^4 \tag{18}$$

where $f^2 = f_1^2 + f_2^2 + f_3^2$ and E(f) is a function which depends on the particular spectral model selected, i.e., Von Karman, Dryden, etc. Interestingly, the coherences coh_{ij}, and the transfer functions H_{ij} are independent of the spectral model selected. The resulting transfer functions and coherences are given by the following equations.

$$H_1 = (E/4\pi f^4)^{1/2}\ (f_2^2 + f_3^2)^{1/2} \tag{19}$$

$$H_{12} = -f_1 f_2/(f_2^2 + f_3^2) \tag{20}$$

$$H_2 = (E/4\pi f^4)^{1/2}\ f\ f_3/(f_2^2 + f_3^2)^{1/2} \tag{21}$$

$$H_{13} = -f_1/f_3 \tag{22}$$

$$H_{23} = -f_2/f_3 \tag{23}$$

$$H_3 = 0 \tag{24}$$

$$coh_{12} = (f_1^2 f_2^2)/(f_2^2 + f_3^2)(f_1^2 + f_3^2) \tag{25}$$

$$coh_{13} = (f_1^2 f_3^2)/(f_2^2 + f_3^2)(f_1^2 + f_2^2) \tag{26}$$

$$coh_{23} = (f_2^2 f_3^2)/(f_1^2 + f_3^2)(f_1^2 + f_2^2) \tag{27}$$

These equations indicate that the three-dimensional transfer functions are realizable for three-dimensional turbulence. In principle, it is possible to use these transfer functions in the system of Figure 3. For isotropic turbulence, the resulting simulation would be the most realistic possible.

SUMMARY AND DIRECTIONS FOR FUTURE RESEARCH

The purpose of this paper is to describe systems for generating multiple turbulence histories with given spectra and cross spectra. Using the systems depicted in Figures 2 and 3, two and three time histories can be generated. For the two time history case, the required transfer functions are always realizable. For the three time history case, small separations in space result in nonrealizable solutions. For realizable cases, once the exact transfer functions are determined, they may be fitted with rational functions as in the VKA method to generate sets of explicit difference equations which may be used to generate sets of turbulence time histories quickly and efficiently. Extensions to four or more time series is straight forward.

Three examples of calculated transfer functions were presented. One was based on the Houbolt and Sen [12] cross spectral model for the vertical velocity component. For this model and small separations, nonrealizable transfer functions occurred. For moderate separations, realizable transfer functions occurred.

The second example model was for longitudinal velocities, separated vertically near the ground. Parameter values were selected as typical for the Cape Canaveral, Florida, area. Because of the strong diagonal dominance of the spectra tensor, no difficulties were encountered.

The third example was for three-dimensional isotropic turbulence based on an arbitrary spectral model. This model yields realizable transfer functions for all situations. The cross spectra for this example were for different velocity components with zero separation.

The system depicted in Figure 3 is not altogether satisfactory since it permits negative values of H_3 [2]. The general problem of Monte Carlo simulation is to simulate a set of N time series with known spectra and cross spectra. If the outputs are to be Gaussian, then all filters are linear. The problem is to find the unknown filter functions from the known spectra and cross spectra. This concept is indicated in Figure 9. The block diagram of Figure 3 is a not quite successful attempt at realizing the system of Figure 9. Future research should be directed toward finding a realization of the general simulation problem.

For the turbulence simulation problem, higher order realizable solutions to the general simulation problem should be found, and if irrational, fitted with stable rational functions as in the VKA method. The resulting stable rational functions can be used to generate stable, explicit difference equations for turbulence generation. These difference equations would be used to efficiently generate the turbulent velocities at several points over the three-dimensional body of an aircraft so that all aerodynamic forces, loads, and moments may be calculated, at least in principle. Only then will the atmospheric simuland be sufficiently accurate that flight simulation engineers can concentrate on other issues.

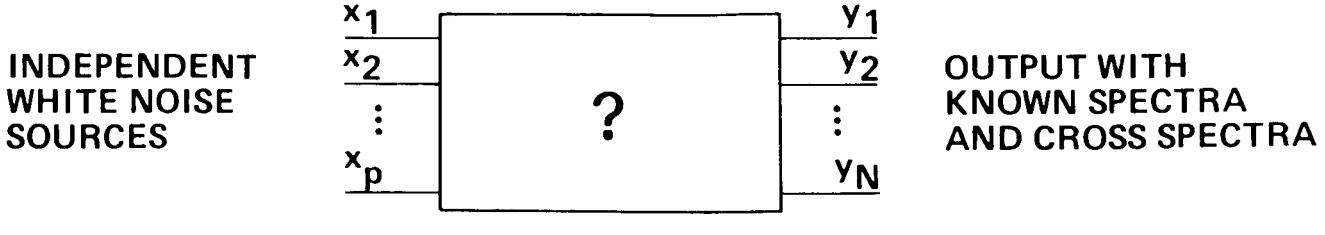

Figure 9. The general Monte Carlo simulation problem.

REFERENCES

1. Frost, W., Wang, S. T., and Camp, D. W.: The Influence of Turbulence Models on Computer-Simulated Landing. AIAA-82-0342, Presented at the AIAA 20th Aerospace Sciences Meeting, January 11-14, 1982, Orlando, Florida.

2. Tatom, F. B., Smith, S. R., Fichtl, G. H., and Campbell, C. W.: Simulation of Atmospheric Turbulent Gusts and Gust Gradients. Journal of Aircraft, Vol. 19, No. 4, April, 1982, pp. 264-271.

3. Camp, D. W., Campbell, W., Frost, W., Murrow, H., and Painter, W.: NASA's B-57B Gust Gradient Program. Journal of Aircraft, Vol. 21, No. 3, March 1984, pp. 175-182.

4. Campbell, C. W. and Sandborn, V. A.: A Spatial Model of Wind Shear and Turbulence. Journal of Aircraft, Vol. 21, No. 12, December 1984, pp. 929-935.

5. Campbell, C. Warren: Monte Carlo Turbulence Simulation Using Rational Approximations to Von Karman Spectra. Submitted to the AIAA Journal, October 1984.

6. Reeves, Paul M.: A Non-Gaussian Turbulence Simulation. Air Force Technical Report AFFDL-TR-69-67, November 1969.

7. Neuman, Frank and Foster, John D.: Investigation of a Digital Automatic Aircraft Landing System in Turbulence. NASA Technical Note D-6066, October 1970.

8. Oldham, Keith B. and Spanier, Jerome: The Fractional Calculus. Academic Press, New York, 1974.

9. Wang, Show-Tien, and Frost, Walter: Atmospheric Turbulence Simulation Techniques With Application to Flight Analysis. NASA Contractor Report 3309, September 1980.

10. Fichtl, G. H., Perlmutter, Morris, and Frost, Walter: Monte Carlo Turbulence Simulation. In Handbook of Turbulence, edited by Walter Frost and Trevor H. Moulden, Plenum Press, New York, 1977.

11. Hoshiya, M. and Tieleman, H. W.: Two Stochastic Models for Simulation of Correlated Random Processes. Virginia Polytechnic Institute Report, VPI-E-71-9, June 1971.

12. Houbolt, John C. and Sen, Asim: Cross-Spectral Functions Bases on Von Karman's Spectral Equation. NASA CR-2011, March 1972.

13. Panofsky, Hans A. and Dutton, John A.: Atmospheric Turbulence. John Wiley and Sons, Inc., New York, 1984.

14. Fichtl, George H., Smith, O. E., Adelfang, Stanley I.: Winds. In NASA Technical Memorandum 82473, June 1982, p. 2.29.

1. REPORT NO.	2. GOVERNMENT ACCESSION NO.	3. RECIPIENT'S CATALOG NO.
NASA TP-2469		

4. TITLE AND SUBTITLE	5. REPORT DATE
Adding Computationally Efficient Realism to Monte Carlo Turbulence Simulation	May 1985
	6. PERFORMING ORGANIZATION CODE
7. AUTHOR(S)	8. PERFORMING ORGANIZATION REPORT #
C. Warren Campbell	
9. PERFORMING ORGANIZATION NAME AND ADDRESS	10. WORK UNIT NO.
George C. Marshall Space Flight Center Marshall Space Flight Center, Alabama 35812	M-485
	11. CONTRACT OR GRANT NO.
	13. TYPE OF REPORT & PERIOD COVERED
12. SPONSORING AGENCY NAME AND ADDRESS	Technical Paper
National Aeronautics and Space Administration Washington, D.C. 20546	14. SPONSORING AGENCY CODE

15. SUPPLEMENTARY NOTES

Prepared by Systems Dynamics Laboratory, Science and Engineering Directorate.

16. ABSTRACT

Frequently in aerospace vehicle flight simulation, random turbulence is generated using the assumption that the craft is small compared to the length scales of turbulence. The turbulence is presumed to vary only along the flight path of the vehicle but not across the vehicle span. The addition of the realism of three-dimensionality is a worthy goal, but any such attempt will not gain acceptance in the simulator community unless it is computationally efficient. A concept for adding three-dimensional realism with a minimum of computational complexity is presented. The concept involves the use of close rational approximations to irrational spectra and cross-spectra so that systems of stable, explicit difference equations can be used to generate the turbulence.

17. KEY WORDS	18. DISTRIBUTION STATEMENT
Monte Carlo Method Simulation Stochastic Processes Atmospheric Turbulence Isotropic Turbulence Low-Level Turbulence Homogeneous Turbulence Gusts	Unclassified - Unlimitd Subject Category 66

19. SECURITY CLASSIF. (of this report)	20. SECURITY CLASSIF. (of this page)	21. NO. OF PAGES	22. PRICE
Unclassified	Unclassified	20	A02

For sale by National Technical Information Service, Springfield, Virginia 22161

NASA-Langley, 1985

National Aeronautics and
Space Administration

Washington, D.C.
20546

Official Business
Penalty for Private Use, $300

THIRD-CLASS BULK RATE

Postage and Fees Paid
National Aeronautics and
Space Administration
NASA-451

NASA

POSTMASTER: If Undeliverable (Section 158 Postal Manual) Do Not Return